

Optical Diagnostics of Zn foil using Non thermal plasma jets (NTPJ) via high voltage

Raneen Qasem Mohammed¹, Baida M. Ahmed²

^{1,2}Department of Physics, College of Science, Mustansiriyah University, Baghdad, Iraq
(aliraneen50@gmail.com¹, dr.baida_222@uomustansiriyah.edu.iq²)

ABSTRACT

The plasma is applied on a zinc (Zn) plate using a Non thermal plasma jets (NTPJ) system that applies different high voltage at gas flow mixture (Ar/O) with a ratio of (10/1) constant at (40)l/min and time exposer 15 sec. Investigated were the optical emission spectroscopy (OES) characteristics of the Ar/O plasma on the Zn plate, when ignited at various high voltage (10, 14, and 18 KV). Using a method based on Stark broadening of the H_{α} line density investigated, it was possible to determine the electron temperature in the range of (1.6-2.9) eV using the Boltzmann method, and the concentration of electrons n_e was determined in the range of $(12.3-9.9) \times 10^{17} \text{cm}^{-3}$ depending on the amount absorbed by the various voltage. Other characteristics of the plasma's parameters have been determined using the (OES) for Ar/O by choosing the strong intensity spectral line's (frequency f_p , Debye length λ_D , and Debye sphere N_D) characteristics. The plasma flame's length was also measured using a ruler, it increased from 1 to 3 cm according to increasing voltage.

Keywords: Non thermal plasma jet (NTPJ), OES, High Voltage, Mixture gases (Ar/O), Zinc plate

1. Introduction

Demand for non-thermal plasma jets (NTPJ) has increased recently as a result of the technologies for a number of biological and industrial applications. Plasma which is generated from ionized gas. This energy may be provided by electricity, radio wave, microwave, or heat [1]. **Cold plasma is produced by electric discharge in a variety of devices, Non-thermal plasma or cold plasma is termed "cold" because the temperature of the electron, ion and others reactive species is near room temperature.**[2] , (NTPJ) is made up of electrons as well as atomic, radical, and ionic excited species with a various of reactive species like positive and negative ions, free radicals, gaseous atoms,

*Corresponding author : Raneen Qasem Mohammed¹
E-mail address: aliraneen50@gmail.com¹

molecules in the base or excited state, and electromagnetic radiation.[3] The system's design and its variables, such as the gas composition, current intensity, humidity, temperature, voltage, and frequency, will have an impact on the cold plasma's composition and effects.[4] Most species created by conventional plasma sources have electronically excited oxygen and nitrogen vibrational modes[5]. Significantly, DBD (Dielectric Barrier Discharge) and Plasma Jet were more commonly being used because of their simpler structure and usability for different purposes [2,6].

The non-thermal plasma jet (NTPJ) has several uses in a variety of crucial industries, including, dentistry [7], photoelectrocatalysis [8], solar cells [9], and sensors [10]. Using argon as a carrier gas, the gas temperature, remains at room. The plasma jet can be touched by hands and directed manually by a user to bring in contact with heat-sensitive objects and materials including skin without causing any heating or painful sensation. NTPJ was created by a high voltage power supply, the discharge was characterized by an optical method.[11]

Moreover, non-thermal plasma jet is an ionized gas produced under atmospheric or low-pressure circumstances [12],The creation of a stable plasma plume is regarded, as an important characteristic of (NTPJ). **Researchers have created a variety of plasma devices based on applied voltage and plasma generating techniques [13]**, including double and single electrode plasma jets and dielectric barrier plasma pencils that are powered by high frequency RF, pulsed, and DC power sources.[14,15] When electrical energy is applied to a flowing gas between the two electrodes (one electrode is covered by dielectric material), a cold atmospheric pressure plasma jet also known as a plasma plume.[16,17].

Reactive oxygen and nitrogen species (RONS), such as OH, NO, and $1O_2$, are created when ionized plasma comes into contact with air (which is made up of O_2 , N_2 , H_2O , etc.). It is believed that the plasma-generated RONS exhibit the same biochemical behavior as reactive species' normal reaction to cells and tissues. RONS can oxidize proteins, lipids, and nucleic acids depending on the biological target qualities and species present. Effects of the plasma composition on cells, tissues.[18-20]

Voltage, current, pressure, and gas flow are some of the variables that affect plasma ionization. In plasma physics and other fields, these elements are crucial, it is essential to have a solid understanding of collisional dynamics, cross sections, and rate coefficients for fundamental processes in both the plasma phase and on surfaces. Plasma plumes are created by plasma jets and can reach distances of several centimeters into the atmosphere around them.[21,22]

In this manuscript, we provided a detailed for the plasma jet and its characterization of the emission spectral after interaction with Zinc plate using both simple homemade devise dependent on the high voltage.

The theoretical part

Optical emission spectroscopy (OES), in general, provides targeted and simple-to-apply measures for plasma diagnostics. is a crucial technique for the analytical characterisation of plasma, including the measurement of frequency f_p , Debye length λ_D , temperature T_e , and electron density n_e . Spectroscopy is very sensitive to the presence of certain elements in the sample and provides outstanding resolution and broad wavelength coverage from (100 to 1025) nm to detect a range of elements.

The Stark broadening of lines is due to the interaction of the charged particles with neutral atoms. Stark broadening, Doppler broadening, and pressure broadening will affect the observed line widths of the plasma spectral. **However, the stark broadening used in the line of research has the greatest impact on the widths of the resulting plasma spectrum**, that is achieved based on the involution of Gaussians, Lorentz, and Stark profiles The perturbation of the electric field affects slightly the selection rules of optical transitions and the atomic level's degeneracy (Stark broadening).[23]

Therefore, these changes result in an alteration of the line shape width, and position. According to the plasma requirement, the controlling interaction of the atom is the stark effect. Thus the analysis of Stark broadening of the plasma spectral line is an ideal tool determining the electron density (n_e) which is given by [24]

$$n_e(\text{cm})^{-1} = \left(\frac{\Delta\lambda}{2\omega_s(\lambda, T_e)} \right) N_r \quad (1)$$

The quantity $\Delta\lambda$ is the FWHM of the line, can be calculated by using equation 2,

$$\Delta\lambda = \left[\frac{\epsilon_0 k_B T_e}{n_e e^2} \right]^{1/2} \cong 7.43 \times 10^2 \left(\frac{T_e(\text{eV})}{n_e} \right)^{1/2} \text{ cm} \quad (2)$$

A theoretically full width Stark Broadening ω_s at the same electron density, $N_r \approx 10^{17} \text{ cm}^{-3}$ is the total population density, ϵ_0 is the permittivity of the vacuum.

The electron temperature of plasma in local thermodynamic equilibrium (LTE) can calculated using Boltzmann relation, a Boltzmann distribution is achieved between energy levels. The radiate transitions should be smaller than collisional transition for achieving (LTE). Electron temperature is defined as[23], **Where the temperature of the electron can be determined by graph slope (fig 3)**

$$\ln\left(\frac{I_{ji} \lambda_{ji}}{h c A_{ji} g_j} \right) = \left(- \frac{E_j}{k T_e} \right) + \ln\left(\frac{N}{U(T)} \right) \quad (3)$$

$U(T)$ partition function, E_j excitation energy of one level (eV), k Boltzmann constant (1.38×10^{-23} J/K), λ_{ji} wavelength corresponding to the transmission between level j and level i , I_{ji} spectral line intensity, g_j density of states, and A_{ji} transition probability between the upper level j and lower level i .

the frequency of oscillation called plasma frequency, which is given by [23],

$$\omega_p = \left(\frac{n_e e^2}{m_e \epsilon_0} \right)^{1/2} \quad (4)$$

e , m_e and n_e is the charge, mass and density of electron respectively. The dimension of the plasma region should be much larger than the Debye length λ_D . The electrons and ions arrange themselves in such a way as to successfully shield any electrostatic fields at a distance of the Debye length. [24], It can be expressed as,

$$\lambda_D = \left(\frac{\epsilon_0 k T}{n_e e^2} \right)^{1/2} \quad (5)$$

Consequently, each charged particle in plasma physics interacts collectively only with the charge particles that lie inside the Debye sphere, and the number of electrons (N_D) is given by [24]:

$$N_D = \frac{4}{3} \pi \lambda_D^3 n_e \quad (6)$$

In this work, diagnostics NTPJ characterization using spectroscopic techniques (OES) for mixture Ar/O₂ gas on the zinc foil in different high voltage, and study the effect of voltage of the transition electrons between Ar/O gas with zinc metal.

Experimental Setup

Materials and equipment

In this experiment, Zinc plates with a total amount of impurity cations $\leq 0.1\%$ and purity $\geq 99.9\%$ were bought from Alfa Aesar (A Johnson Matthey) Company (Germany), and to prepare it ,one piece was cut with dimensions of length , width, and thickness (1cm , 1 cm , 0.25 mm) respectively, washed with ethanol and then with distilled water well to remove impurities and then dried in air . working in a 37C⁰ ambient temperature and ordinary atmospheric pressure environment. The power source for plasma formation was a high voltage AC generator (Trek, MODEL 615- 10, USA) with a frequency 50Hz and a constant flow gas (40) l/min and time Exposing (15)sec with different high voltage (10, 14, and 18)kv.

The schematic view of the experimental setup and diagnostic arrangement is shown in Figure 1 A different high-voltage (HV) (Fanavaran Nano- Meghyas HV35P OV) source is used to produce plume (1-3) cm connected with electrode (10 cm Made of copper) is placed **inside a quartz tube that is (10) cm long and (7, 10) mm inner and outer diameter respectively and 1mm thickness is used in this work. Edge fixed at 3mm between the high voltage electrode's tip and the gas entrance end of the tube. The HV electrode is connected to a pulsed Ac power supply, repetition rate is 50 Hz. The optical emission spectroscopy (OES) from the CAPPJ was collected by an (Ocean Optics spectrometer, Flame-S-XR1)**

using a fiber probe connected lens. And the other side was connected with computer to appear the spectra.

In the current study, the Ar cold atmospheric pressure plasma jet system is mainly composed of a voltage controller, electrodes, dielectrics and Argon gas. The design of the NTPJ as can be seen in Fig. 1

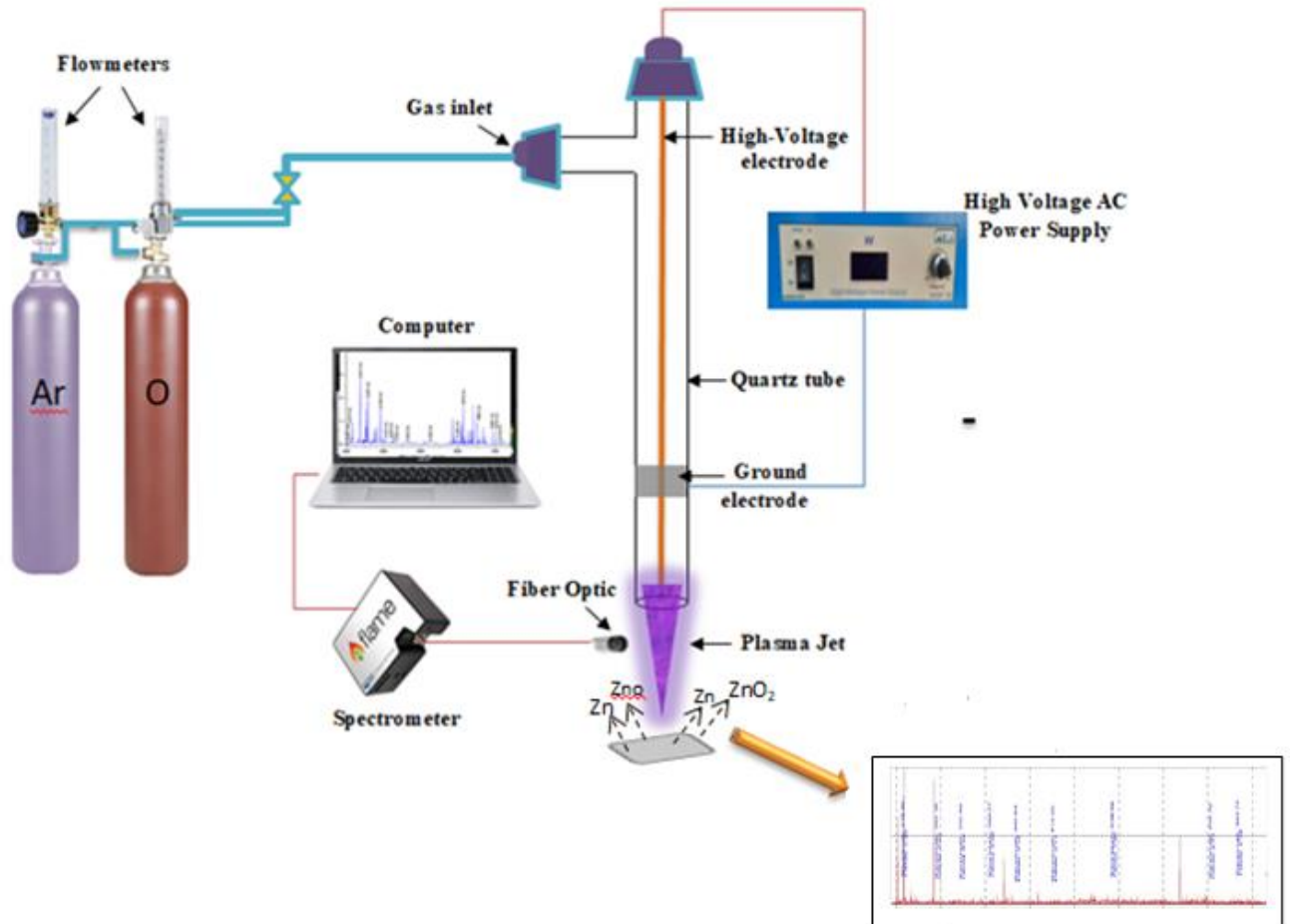


Fig. 1 Schematic of plasma generates.

The high voltage system is liable for production the gas to the plasma jet and the change in the voltage **effect** on the plume plasma, where increases in the voltage cause to increase the length of plume. In this work, Argon gas with a commercial grade of 99.99% was used to operate the plasma jet system mixture with Oxygen at ratio ($Ar_{(10)}/O_{(1)}$). The Argon flow was controlled by the flowmeter. Once the Argon gas is introduced through the two electrodes and the suitable high voltage is applied between them (10, 14, and 18)kv, the argon atoms are ionized by driving off electrons so that the ionization of neighboring Argon species occurred by a collision with free electrons. After the series of these reactions, the Argon gas converts to the plasma state.

Photon emission in this region is discovered by an optical emission spectrometer. The measurement of the vibrational and electron temperatures within the plasma is made possible by the spectra, which offer useful information on the species present in the plasma and their electron excitation. An instrument called a spectrometer, which comprises of a lens and a detector coupled by a fiber optic cable, was used to collect the UV-visible emission spectra from the plasma reactor. Spectroscopy with the model number HR4000CG-UV-NIR (Ocean Optics) model number was used. When mixed Ar/O gas is fed through the electrode at a flow rate of (40 l/min), and apply different voltages at (10,14,18 KV) a homogenous plasma plume is created both inside the tube and in the surrounding air. Zinc foil with dimensions of 1 cm in length, 1 cm, and 0.15 mm in thickness is used to explore the impacts of zinc's plasma optical emission and the emission of other factors.

Results and Discussion

In this study, the plasma generation system was designed and manufactured using different voltages are applied to both ends of the plasma tube ,and the thermal and optical properties of non-thermal plasma were studied because they are of great important in plasma formation ,it was demonstrated from the study of thermal properties by studying the effect of applied voltage .

By increasing the voltage, a number of secondary electrons are released , and bombardment with electrons , photons, and neutral atoms contributes to this process. As a result of the acceleration of the secondary electrons and their collision with gas atoms, the temperature increases but but stay within at room temperature. Also, the length of the generated plasma plume is increases with the increase of applied voltage. NIST [25] was used to compare the spectral lines produced by Ar, O and Zn electron transitions mission spectra of plasma spectral for Ar/O₂ mixture gas with different voltages.as shown in figure 2,

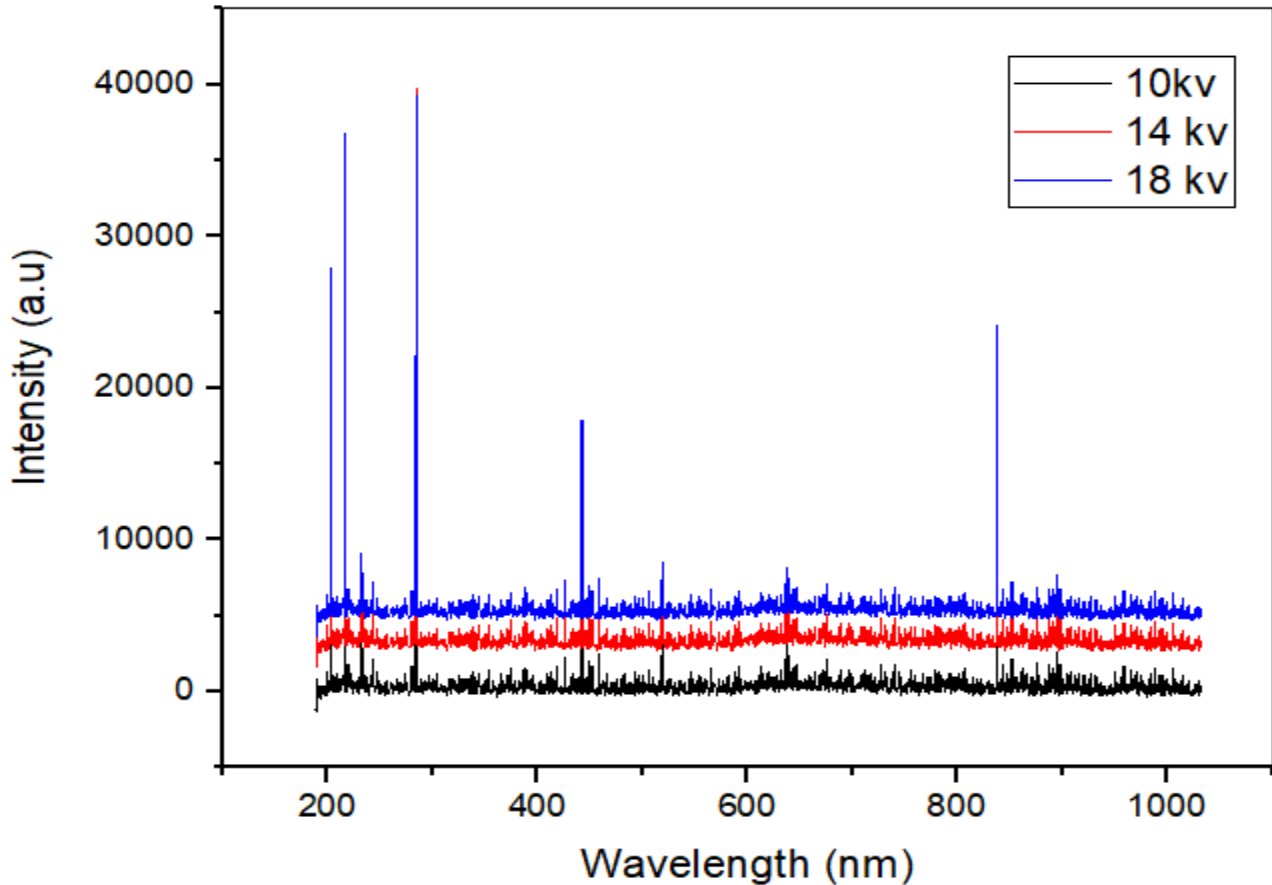


Fig. 2 Emission spectra of Non-thermal plasma jets (NTPJ) for Ar/O2 mixture gas with different voltage (the inset represent cold plasma at 10,14, and 18kv)

The highest peak of intensity at (Ar II) wavelength 284.53 nm at peak 34283.4 and the transitions $3s^2 3p^4(^3p)4s-3s^2 3p^4(^1D)4p$. The other parameters determined it by depending on NIST technology, as in the Table 1.

Table1: Spectroscopic data, of the relevant atomic argon (Ar/O) on the Zinc plate emission spectral lines, lower and upper energy, and transition energy levels at different voltage applies.

IONS	Wavele ngth λ (nm)	gk Aki (S-I)	Ei (eV)	EK(eV)	Transitions	
					Lower level	Upper level
Ar II	202.87	6.7e+07	19.7622610	25.87220	$3s^2 3p^4(^3p)4p$	$3s^2 3p^4(^3p)6d$

Ar IV	206.13	6.7e+07	31.906537	37.917765	$3s^2 3p^2 (^3p) 4s$	$3s^2 3p^2 (^1D) 4f$
Ar II	215.89	6.7e+07	18.060639	23.8081844	$3s^2 3p^4 (^3p) 3d$	$3s^2 3p^4 (^1s) 4p$
Ar II	221.92	6.7e+07	18.732439	24.3156696	$3s^2 3p^4 (^3p) 3d$	$3s^2 3p^4 (^3p_1) 4f$
Ar II	232.11	5.6e+07	19.680048	25.0177619	$3s^2 3p^4 (^3p) 4p$	$2s^2 3p^4 (^3p) 5d$
Ar III	242.74	2.7e+08	29.792457	34.8984141	$3s^2 3p^3 (^2p^0) 4p$	$3s^2 3p^3 (^2p^0) 4d$
ArII	249.19	2.7e+08	19.7622610	24.737977	$3s^2 3p^4 (^3p) 4p$	$3s^2 3p^4 (^1D) 4d$
Ar IV	261.16	1.7e+08	31.2399	35.98660	$3s^2 3p^2 (^3p) 4s$	$3s^2 3p^2 (^3p) 4p$
ArII	274.01	2.9e+08	21.351799	25.874898	$3s^2 3p^4 (^1D) 4p$	$3s^2 3p^4 (^3p) 6d$
Ar IV	279.96	4.4e+08	31.022731	35.454050	$3s^2 3p^2 (^3p) 4s$	$3s^2 3p^2 (^3p) 4p$
Ar II	284.53	1.0e+06	17.1400274	21.99804	$3s^2 3p^4 (^3p) 4s$	$3s^2 3p^4 (^1D) 4p$
Ar II	296.85	2.1e+08	21.3668910	25.553574	$3s^2 3p^4 (^1D) 3d$	$3s^2 3p^4 (^3p_1) 5f$
Ar III	302.31	1.8e+09	25.69361	29.792457	$3s^2 3p^3 (^2p^0) 4s$	$3s^2 3p^3 (^2p^0) 4p$
ArII	324.55	2.112e+08	19.261084	23.082303	$3s^2 3p^4 (^3p) 4p$	$3s^2 3p^4 (^3p) 4d$
ArII	337.2	3.5e+07	21.4281461	25.1027300	$3s^2 3p^4 (^1D) 3d$	$3s^2 3p^4 (^3p) 6p$
ArII	352.51	1.82e+08	21.4924023	25.0101830	$3s^2 3p^4 (^1D) 4p$	$3s^2 3p^4 (^3p) 5d$
ArII	364.17	8.4e+08	21.3517998	24.757145	$3s^2 3p^4 (^1D) 4p$	$3s^2 3p^4 (^1D) 4d$
Ar II	374.47	1.3e+07	19.762261	23.070289	$3s^2 3p^4 (^3p) 4p$	$3s^2 3p^4 (^3p) 4d$
Ar II	388.74	4.64e+07	21.498049	24.690028	$3s^2 3p^4 (^1D) 4p$	$3s^2 3p^4 (^3p) 4d$
ArII	407.83	4.76e+07	18.454114	21.992402	$3s^2 3p^4 (^1D) 4s$	$3s^2 3p^4 (^1D) 4p$
Ar III	417.56	8.7e+05	25.748138	28.718133	$3s^2 3p^3 (^2p^0) 4s$	$3s^2 3p^3 (^2D^0) 4p$
ArII	425.51	8.4e+06	19.680048	22.592663	$3s^2 3p^4 (^3p) 4p$	$3s^2 3p^4 (^3p) 4s$
Ar II	457.98	1.6e+08	17.265833	19.972538	$3s^2 3p^4 (^3p) 4s$	$3s^2 3p^4 (^3p) 4p$
Ar VIII	464.35	3.6e+05	134.7535	137.4204	$2p^6 10g$	$2p^6 12h$

<i>Ar II</i>	480.63	4.68e+08	16.64385	19.2229021	$3s^2 3p^4 ({}^3p)4s$	$3s^2 3p^4 ({}^3p)4p$
<i>Ar II</i>	506.58	8.92e+07	16.812472	19.2610841	$3s^2 3p^4 ({}^3p)4s$	$3s^2 3p^4 ({}^3p)4p$
<i>Ar II</i>	518.2	1.2e+06	23.4380888	25.8295177	$3s^2 3p^4 ({}^3p)5p$	$3s^2 3p^4 ({}^3p)7s$
<i>Ar II</i>	530.63	2.7e+05	19.972538	22.3087048	$3s^2 3p^4 ({}^3p)4p$	$3s^2 3p^4 ({}^1s)3d$
<i>Ar II</i>	545.57	2.4e+06	23.6304249	25.9020761	$3s^2 3p^4 ({}^3p)4d$	$3s^2 3p^4 ({}^3p_2)7p$
<i>Ar I</i>	565.1	3.2e+06	12.907015	15.100543	$3s^2 3p^5 ({}^2p^0)4p$	$3s^2 3p^5 ({}^2p^0)5d$
<i>ArII</i>	592.09	3.15e+06	24.15972864	26.2550761	$3s^2 3p^4 ({}^3p_2)4f$	$3s^2 3p^4 ({}^3p_1)6g$
<i>Ar II</i>	613.01	4.8e+06	17.7430910	19.7622610	$3s^2 3p^4 ({}^3p)3d$	$3s^2 3p^4 ({}^3p)4p$
<i>Ar II</i>	637.94	1.3e+06	19.6800489	21.6240706	$3s^2 3p^4 ({}^3p)4p$	$3s^2 3p^4 ({}^1D)3d$
<i>Ar I</i>	658.96	9.1e+04	13.0948725	14.9715223	$3s^2 3p^5 ({}^2p^0)$	$3s^2 3p^5 ({}^2p^0)4d$
<i>Ar II</i>	675.76	8.0e+06	17.775792	19.6103078	$3s^2 3p^4 ({}^3p)3d$	$3s^2 3p^4 ({}^3p)4p$
<i>Ar I</i>	696.11	1.2e+06	13.17177770	14.9526045	$3s^2 3p^5 ({}^2p^0)4p$	$3s^2 3p^5 ({}^2p^0)4d$
<i>Ar I</i>	727.17	7.7e+05	13.0757157	14.780512	$3s^2 3p^5 ({}^2p^0)4p$	$3s^2 3p^5 ({}^2p^0)4d$
<i>Ar I</i>	739.17	2.2e+06	13.1717777	14.848368	$3s^2 3p^5 ({}^2p^0)4p$	$3s^2 3p^5 ({}^2p^0)6s$
<i>Ar II</i>	783.14	4.4e+05	24.3780167	25.9594655	$3s^2 3p^5 ({}^2p_0)4f$	$3s^2 3p^5 ({}^3p)6d$
<i>Ar I</i>	801.54	4.6e+07	11.5483544	13.094872	$3s^2 3p^5 ({}^2p^0)4s$	$3s^2 3p^5 ({}^2p^0)4p$
<i>Ar II</i>	817.87	9.9e+04	23.89325004	25.4080133	$3s^2 3p^4 ({}^3p)4d$	$3s^2 3p^4 ({}^3p)6p$
<i>Ar II</i>	830.23	4.59e+07	23.570177223	25.0641424	$3s^2 3p^4 ({}^3p)5p$	$3s^2 3p^4 ({}^3p)5d$
<i>Ar II</i>	837.55	4.59e+07	24.16242396	25.6423388	$3s^2 3p^4 ({}^3p_2)4f$	$3s^2 3p^4 ({}^3p_0)5g$
<i>Ar I</i>	851.35	4.17e+07	11.82807116	13.2826390	$3s^2 3p^5 ({}^2p^0)4s$	$3s^2 3p^5 ({}^2p^0)4p$
<i>Ar I</i>	860.51	5.2e+06	13.30222747	14.742540	$3s^2 3p^5 ({}^2p^0)4p$	$3s^2 3p^5 ({}^2p^0)4d$
<i>Ar II</i>	875.31	1.27e+06	22.266598	23.6825223	$3s^2 3p^4 ({}^1s)3d$	$3s^2 3p^4 ({}^3p)5p$
<i>Ar II</i>	887.01	1.4e+06	23.6203867	25.0177617	$3s^2 3p^4 ({}^3p)5p$	$3s^2 3p^4 ({}^3p)5d$
<i>Ar II</i>	894.53	1.0e+06	22.77287965	24.15972864	$3s^2 3p^4 ({}^3p)4d$	$3s^2 3p^4 ({}^3p)4f$
<i>Zn I</i>	232.11	2.14e+09	4.00609281	9.312557	$3d^{10} 4s4p$	$3d^{10} 4s14d$

Zn	242.74	2.14e+09	4.00609281	9.11289	3d ¹⁰ 4s4p	3d ¹⁰ 4s7f
Zn I	274.01	7.04e+07	4.00609281	8.5343044	3d ¹⁰ 4s4p	3d ¹⁰ 4s4f
Zn I	284.53	8.74e+06	4.07788079	8.4435502	3d ¹⁰ 4s4p	3d ¹⁰ 4s6p
Zn I	303.68	8.74e+06	4.02965990	8.1125699	3d ¹⁰ 4s4p	3d ¹⁰ 4s6s
Zn I	352.51	1.4e+07	4.07788079	7.6040557	3d ¹⁰ 4s4p	3d ¹⁰ 4s5d
Zn I	388.74	1.4e+07	5.7956913	8.990962	3d ¹⁰ 4s4p	3d ¹⁰ 4s7d
Zn I	457.98	3.12e+07	6.65450963	9.363060	3d ¹⁰ 4s5s	3d ¹⁰ 4s32p
Zn I	506.15	2.18e+09	6.65450963	9.099924	3d ¹⁰ 4s5s	3d ¹⁰ 4s9p
Zn I	518.2	2.18e+09	5.7956913	8.1876271	3d ¹⁰ 4s4p	3d ¹⁰ 4s6s
Zn I	530.63	2.18e+09	6.65450963	8.989370	3d ¹⁰ 4s5s	3d ¹⁰ 4s8p
Zn II	619.68	1.71e+07	6.119245	8.113729	3d ¹⁰ 4p	3d ¹⁰ 4s ²
Zn I	637.94	2.4e+08	5.7956913	7.7438711	3d ¹⁰ 4s4p	3d ¹⁰ 4s4d
O II	208.92	2.68e+07	26.2254001	32.147624	3s ² 2p ² (³ p)3p	3s ² 2p ² (¹ D)4s
O III	255.18	6.90e+08	41.140615	45.986014	3s ² 2p ² (² p ⁰)3d	3s ² 2p ² (² p ⁰)4p
O II	273.55	2.37e+08	25.2856211	29.820351	3s ² 2p ² (³ p)3p	3s ² 2p ² (³ p)4s
O II	279.96	2.01e+06	29.820351	34.252347	3s ² 2p ² (³ p)4s	3s ² 2p ² (¹ D)4f
O II	296.85	9.15e+08	30.811970	34.990808	3s ² 2p ² (¹ D)4p	3s ² 2p ² (¹ s)4s
O II	315.94	1.97e+07	28.591928	32.519421	3s ² 2p ² (¹ s)3s	3s ² 2p ² (³ p)5p
O II	337.2	3.18e+07	28.7060920	32.382266	3s ² 2p ² (³ p)3d	3s ² 2p ² (³ p)5p
O II	343.96	8.07e+07	28.8307832	32.436939	3s ² 2p ² (³ p)3d	3s ² 2p ² (³ p)5p
O II	364.17	7.56e+06	29.0686699	32.467735	3s ² 2p ² (¹ D)4p	3s ² 2p ² (³ p)5p
O II	374.02	3.60e+07	28.361069	31.673760	3s ² 2p ² (⁴ p)3p	3s ² 2p ² (⁴ p)3d
O II	388.74	6.42e+07	25.6650368	28.8570199	3s ² 2p ² (⁴ p)3p	3s ² 2p ² (⁴ p)3d
O II	411.37	1.45e+08	28.361069	31.718825	3s ² 2p ² (¹ D)3p	3s ² 2p ² (¹ D)3d
O II	425.51	1.9e+06	31.319581	34.233210	3s ² 2p ² (¹ D)3d	3s ² 2p ² (¹ D)4f

<i>O II</i>	432.11	1.12e+08	28.8832609	31.7508339	$3s^2 2p^2 ({}^3p) 3d$	$3s^2 2p^2 ({}^3p) 4f$
<i>O II</i>	492.76	3.26e+08	26.3047208	28.8217045	$3s^2 2p^2 ({}^3p) 3p$	$3s^2 2p^2 ({}^3p) 3d$
<i>O II</i>	506.58	5.90e+05	26.2490334	28.6934114	$3s^2 2p^2 ({}^3p) 3p$	$3s^2 2p^2 ({}^3p) 3d$
<i>O II</i>	580.73	2.10e+06	26.379157	28.51245	$3s 2p^4$	$3s^2 2p^2 ({}^1D) 3p$
<i>O II</i>	611.34	1.46e+07	29.586034	31.613683	$3s^2 2p^2 ({}^3p) 4s$	$3s^2 2p^2 ({}^5s^0) 3s$
<i>O II</i>	727.17	2.87e+06	28.8568239	30.5600365	$3s^2 2p^2 ({}^3p) 3d$	$3s^2 2p^2 ({}^3p) 4p$
<i>O II</i>	755.5	4.44e+06	28.8630624	30.5637449	$3s^2 2p^2 ({}^3p) 3d$	$3s^2 2p^2 ({}^3p) 4p$
<i>O II</i>	860.2	1.51e+08	28.941697	30.380752	$3s^2 2p^2 ({}^3p) 3d$	$3s^2 2p^2 ({}^3p) 4p$

After knowing the values of the energies of higher Levels ,we can obtain the statistical weights and transition probabilities that were used for the experimental plots for the gases (Ar/O) and Zn metal. Also, we can use eq.3 to acquire the electron temperature which it equals the slope of the fitted line $1/KBT$. R^2 is the statistical coefficient for evaluating the quality of a linear fit, known as the fitting lines, ranges in value from (0.8 to 0.9). Equation (1), which accounts for the sharp broadening in plasmas as the result of collisions with charged species, is

Use to compute the electron densities.

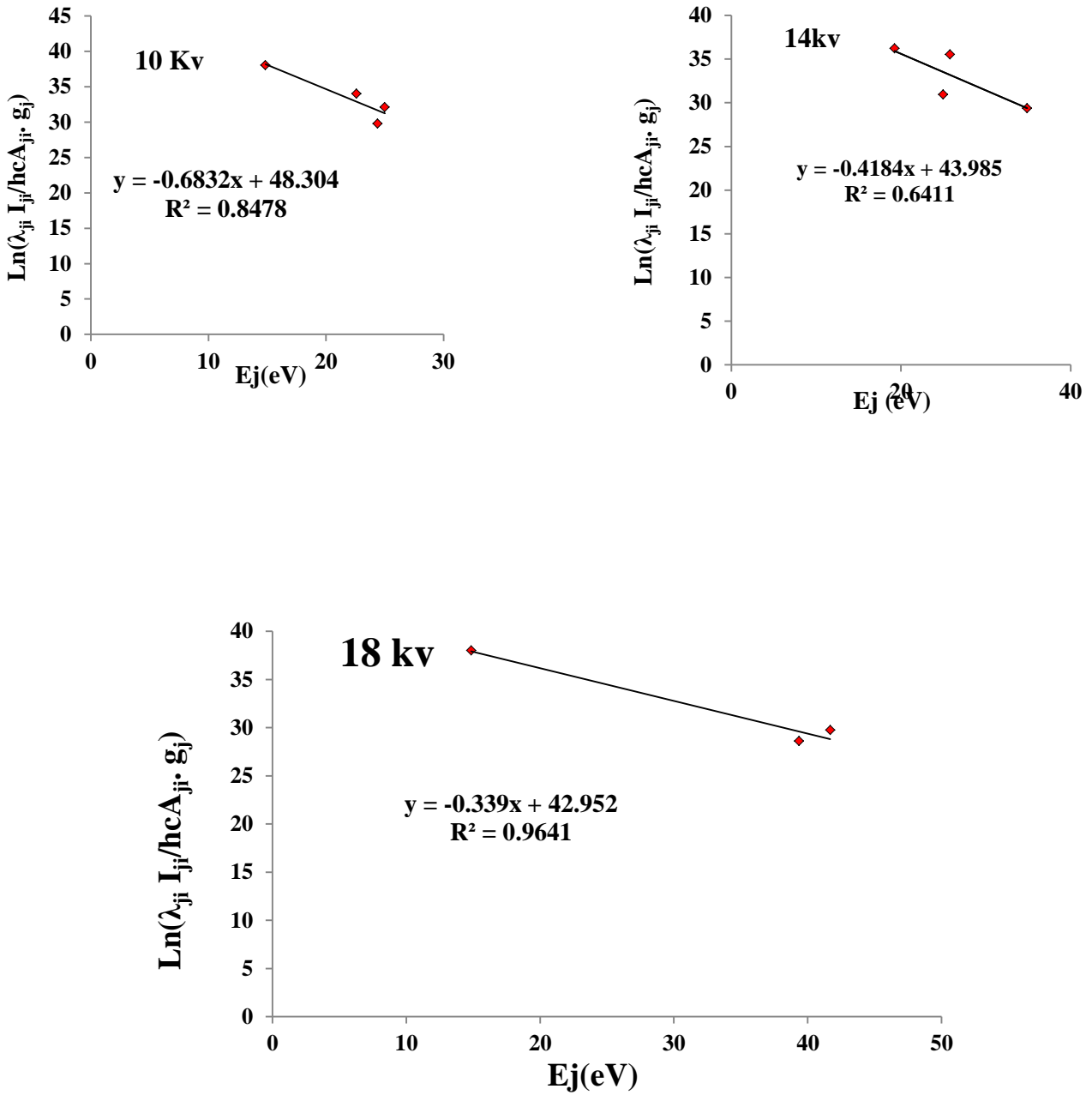


Fig. 3 Boltzmann plot for the Ar/O with different voltages (10, 14 and 18) kv using CAPPJ.

Table 2. it shows us that increasing the voltage leads to an increase in the electron density n_e , Which in turn increases the electron temperature T_e , but the number of electron N_D is decreases with increasing voltage.

Table 2 Plasma parameters (T_e , n_e , f_p , λ_D , and N_D) for the Argon (Ar) with different voltage values.

V (kV)	T_e (eV)	$n_e \cdot 10^{17}$ (cm^{-3})	f_p (Hz) $\cdot 10^{12}$	$\lambda_D \cdot 10^{-5}$ (cm)	$N_d \cdot 10^3$
10	1.600	12.30	9.959	0.847	3.135
14	2.300	10.20	9.069	1.111	5.862
18	2.900	9.90	8.935	1.267	8.425

Fig. 4 shows the variation of electron density (n_e) calculated by stark broadening using equation (1) and electron temperature (T_e) calculated by Boltzmann plot using eq. (3), from this figure notice that the electron density decreasing from $(12.30-9.9) \times 10^{17} \text{cm}^{-3}$ and electron temperature increasing (1.6-2.9) eV with increases applying voltage. This is due the interactions atoms Ar/O with atoms of zinc surface. Cause to highest electron temperature.

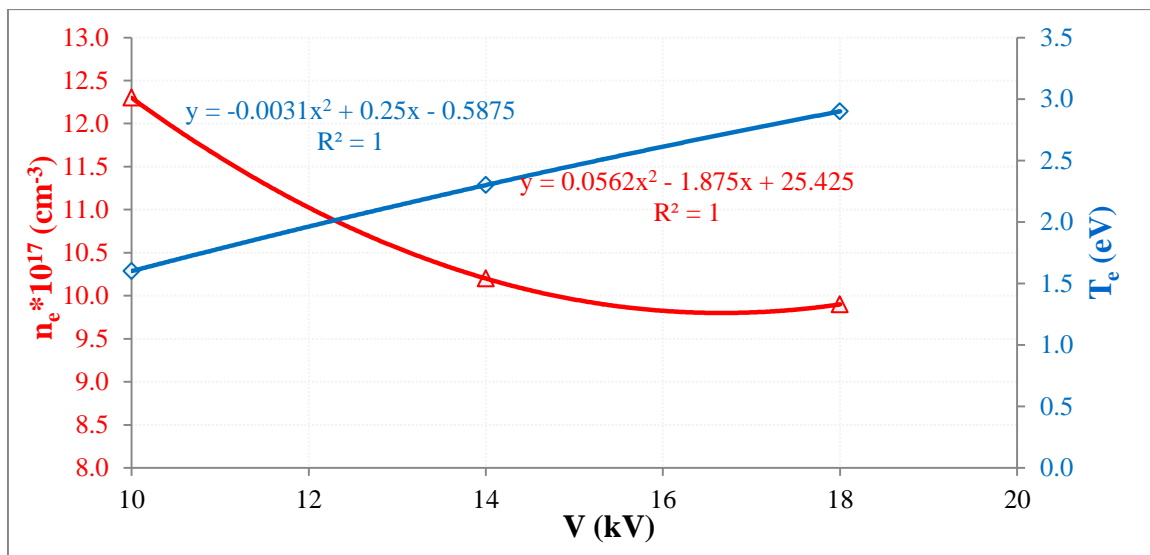


figure 4 Variation of (T_e) and (n_e) versus the applying voltage (10, 14, and 18) KV. at constant gas flow 40 l/min.

Conclusion

Non-thermal plasma jet (NTPJ) is used to bombard the zinc target, this technique allowed for the calculation of plasma parameters such as density n_e , and temperature T_e of electrons based on the experimental results of the optical emission spectrum (OES), by connecting them with Boltzmann's plot and the Stark broadening. Were obtained from the target with different voltage values and for each requirement T_e and n_e were estimated. In this study, it was also concluded how different voltages affect the length of the plasma plume, it increases with the increase in the value of the applied voltage. The voltage applied to the gas Ar/O leads to an increase in the movement of its electrons and the length of its plasma plume is longer, which leads to a rise in its temperature and thus its ionization and transformation into plasma intensity. In addition to the zinc plate being oxidized and transformed into Zinc oxide.

Acknowledgment

The authors are grateful for support from the Physics department/college of science Mustansiriyah University and Lab. of Plasma while doing this study.

References

- [1] Nehra, V., Kumar, A., & Dwivedi, H. K. (2008). Atmospheric non-thermal plasma sources. *International Journal of Engineering*, 2(1), 53-68.
- [2] Tiwari, S., Sharma, M., Panier, S., Mutel, B., Mitschang, P., & Bijwe, J. (2011). Influence of cold remote nitrogen oxygen plasma treatment on carbon fabric and its composites with specialty polymers. *Journal of Materials Science*, 46, 964-974.
- [3] Scholtz, V., Pazlarova, J., Souskova, H., Khun, J., & Julak, J. (2015). Nonthermal plasma—A tool for decontamination and disinfection. *Biotechnology advances*, 33(6), 1108-1119.
- [4] Francis F. Chen, "introduction to plasma physics and controlled fusion", Third edition, Springer international publication Switzerland 2016.
- [5] Pandiyaraj, K. N., Kumar, A. A., RamKumar, M. C., Deshmukh, R. R., Bendavid, A., Su, P. G., ... & Gopinath, P. (2016). Effect of cold atmospheric pressure plasma gas composition on the surface and cyto-compatible properties of low density polyethylene (LDPE) films. *Current Applied Physics*, 16(7), 784-792.
- [6] Xiong, Q., Lu, X., Ostrikov, K., Xiong, Z., Xian, Y., Zhou, F., ... & Jiang, Z. (2009). Length control of He atmospheric plasma jet plumes: Effects of discharge parameters and ambient air. *Physics of Plasmas*, 16(4).
- [7] Hoffmann, C., Berganza, C., & Zhang, J. (2013). Cold Atmospheric Plasma: methods of production and application in dentistry and oncology. *Medical gas research*, 3(1), 1-15.
- [8] Garcia-Segura, S., & Brillas, E. (2017). Applied photoelectrocatalysis on the degradation of organic pollutants in wastewaters. *Journal of Photochemistry and Photobiology C: Photochemistry Reviews*, 31, 1-35.
- [9] Luo, J., Wang, Y., & Zhang, Q. (2018). Progress in perovskite solar cells based on ZnO nanostructures. *Solar Energy*, 163, 289-306.
- [10] Khalaf, M. A., Ahmed, B. M., & Aadim, K. A. (2020). Spectroscopic analysis of CdO1-X: SnX plasma produced by Nd: YAG laser. *Iraqi Journal of Science*, 1665-1671.
- [11] Ahmed, B. M. (2020, November). Plasma parameters generated from iron spectral lines by using LIBS technique. In *IOP Conference Series: Materials Science and Engineering* (Vol. 928, No. 7, p. 072096). IOP Publishing.

- [12] Simoncelli, E., Stancampiano, A., Boselli, M., Gherardi, M., & Colombo, V. (2019). Experimental investigation on the influence of target physical properties on an impinging plasma jet. *Plasma*, 2(3), 369-379.
- [13] Chi-Feng Su , Chih-Tung Liu , Jong-Shinn Wu and Ming-Tzu Ho , Development of a High-Power-Factor Power Supply for an Atmospheric-Pressure Plasma Jet , . *Electronics* , 31 August 2021. <https://doi.org/10.3390/>
- [14] Guo LiGuo LiHe-Ping LiHe-Ping LiWenting SunWenting Sun, Discharge Features of Radio-Frequency, Atmospheric-Pressure Cold Plasmas Under an Intensified Local Electric Field, *Journal of Physics D Applied Physics* 41(20):202001Follow journal September 2008, DOI: 10.1088/0022-3727/41/20/202001
- [15] Sultan, M. S. (2018). Effect of gas pressure and flow rate on the plasma power and deposition rate in magnetron sputtering system. *Research Journal of Nanoscience and Engineering*, 2(1), 1-8.
- [16] Mansour, S. A. (2015). Self-absorption effects on electron temperature-measurements utilizing laser induced breakdown spectroscopy (LIBS)-techniques. *Optics and Photonics Journal*, 5(03), 79.
- [17] Nikiforov, A. Y., Leys, C., Gonzalez, M. A., & Walsh, J. L. (2015). Electron density measurement in atmospheric pressure plasma jets: Stark broadening of hydrogenated and non-hydrogenated lines. *Plasma Sources Science and Technology*, 24(3), 034001.
- [18] E. Gillian, A. Casey, V. Milosavljevic, Y. Liu, O. Howe, J. Patrick, F., “Non-thermal Atmospheric Plasma Induces ROS-independent Cell Death in U373MG Glioma Cells and Augments the Cytotoxicity of Temozolomide”, *British journal of cancer BJC*, 114, 435–443 (2016)
- [19] von Woedtke, T., Schmidt, A., Bekeschus, S., Wende, K., & Weltmann, K. D. (2019). Plasma medicine: A field of applied redox biology. *In vivo*, 33(4), 1011-1026.
- [20] Torres, J., Palomares, J. M., Sola, A. J. A. M., Van der Mullen, J. J. A. M., & Gamero, A. (2007). A Stark broadening method to determine simultaneously the electron temperature and density in high-pressure microwave plasmas. *Journal of Physics D: Applied Physics*, 40(19), 5929.
- [21] Fricke, K., Steffen, H., Von Woedtke, T., Schröder, K., & Weltmann, K. D. (2011). High rate etching of polymers by means of an atmospheric pressure plasma jet. *Plasma Processes and Polymers*, 8(1), 51-58.
- [22] Sultan, M. S. (2018). Effect of gas pressure and flow rate on the plasma power and deposition rate in magnetron sputtering system. *Research Journal of Nanoscience and Engineering*, 2(1), 1-8.
- [23] Torres, J., Palomares, J. M., Sola, A. J. A. M., Van der Mullen, J. J. A. M., & Gamero, A. (2007). A Stark broadening method to determine simultaneously the electron temperature and density in high-pressure microwave plasmas. *Journal of Physics D: Applied Physics*, 40(19), 5929.
- [24] Nikiforov, A. Y., Leys, C., Gonzalez, M. A., & Walsh, J. L. (2015). Electron density measurement in atmospheric pressure plasma jets: Stark broadening of hydrogenated and non-hydrogenated lines. *Plasma Sources Science and Technology*, 24(3), 034001.
- [25] National Institute of Standards and Technology (NIST) Atomic Spectra Database ,(Version 5). Available ay <http://physics.nist.gov/asd3>, last updated: September 16,(2022.)